Desalination and Water Treatment
www.deswater.com
doi: 10.1080/19443994.2015.1055311

57 (2016) 11361–11374
May

Taylor & Francis
Taylor & Francis Group

Isotherm, kinetics, and process optimization for removal of Remazol Brilliant Blue dye from contaminated water using adsorption on acid-treated red mud

G.M. Ratnamala[a,b], Shetty K. Vidya[b,*], G. Srinikethan[b]

[a]*Department of Chemical Engineering, KLE Dr M S Sheshagiri College of Engineering and Technology, Udyambag, Belgaum 590008, Karnataka, India, Tel. +91 824 2474000, extn. 3606; Fax: +91 824 2474033; email: ratna_chem@yahoo.com (G.M. Ratnamala)*

[b]*Department of Chemical Engineering, National Institute of Technology Karnataka, Srinivasnagar Post, Surathkal 575025, Karnataka, India, emails: vidyaks68@yahoo.com, vidyaks95@nitk.ac.in (Shetty K. Vidya), srinikethan.g@gmail.com (G. Srinikethan)*

Received 7 January 2015; Accepted 13 April 2015

ABSTRACT

Red mud, which is a waste product from alumina production, has been utilized after activation with concentrated sulphuric acid treatment for removal of Remazol Brilliant Blue (RBB) dye from dye-contaminated water to investigate its potential as a low-cost adsorbent. The activation has enhanced the surface area of red mud from 20.2 to 32.28 m^2/g, thus enhancing its adsorption capacity. The effect of initial dye concentration, contact time, initial pH and adsorbent dosage on percentage removal of dye using concentrated sulphuric acid-treated red mud (CATRM) was investigated. The ranges of these variables for optimization were selected based on batch studies. Acidic pH favoured adsorption and 300 min contact time was found to be suitable for attainment of equilibrium under shaking conditions of 145 rpm. Langmuir isotherm model has been found to represent the equilibrium data for RBB-CATRM adsorption system better in comparison with Freundlich model. The adsorption capacity of CATRM was found to increase with the increase in temperature, and at 40°C, it was found to be 125 mg dye/g of CATRM. The adsorption kinetics was represented by second-order kinetic model, and the kinetic constant was estimated to be 0.0063 g/mg min. Factors affecting the adsorption process were optimized by response surface methodology based on experiments designed as per central composite design. The effects of individual variables and their interaction effects on dye removal were determined. The results of the study showed that dye removal efficiency of almost 100% can be obtained with optimal conditions of initial dye concentration at 105 mg/l, red mud dosage of 2.05 g/l, initial pH of 1 and temperature of 31.65°C. pH and temperature were found to have high interaction effect on adsorption.

Keywords: Adsorption; Isotherm; Kinetics; Red mud; Remazol Brilliant Blue; Response surface methodology

1. Introduction

Dyes are used in dyeing, paper and pulp, textiles, plastics, leather, cosmetic and food industries [1], and effluents from these industries contain the residual dyes. The receiving water bodies also undergo chemical and biological changes that consume dissolved oxygen and thereby kills the aquatic organisms [2]. Increasing environmental pollution-related problems by toxic dyes due to their hazardous nature is a

*Corresponding author.

matter of great concern. These dye compounds are aesthetically displeasing and also inhibit sunlight penetration into the water and affect the aquatic ecosystem. Remazol Brilliant Blue (RBB), which is also called as Reactive Blue 220, is a water soluble reactive dye, which is widely used in the textile industries for dyeing cotton fabric. RBB is one of the important dyes in the textile industry with the molecular name Cuprate(4-), [4,5-dihydro-4-[[8-hydroxy-7-[[2-hydroxy-5-methoxy-4-[[2-(sulfooxy)ethyl]sulfonyl]phenyl]azo]-6-sulfo-2-naphthalenyl]azo]-5-oxo-1-(4-sulfophenyl)-1H-pyrazole-3-carboxylato(6-)]-, sodium, and it is a vinyl sulphone-based formazan dye [3], a special class of azo dye containing Cu. Dyes and their breakdown products are toxic, carcinogenic or mutagenic to life forms mainly because of carcinogens, such as benzidine, naphthalene and other aromatic compounds [4,5]. Moreover, Remazol Brilliant Blue, BB, contains a copper complex, and copper may bioaccumulate in the human body, aquatic life, natural water bodies and also possibly trapped in the soil leading to toxicity [6], if the dye is released with effluent water.

There are various conventional methods of removing dyes from dye wastewater which include coagulation and flocculation, oxidation [7], electrochemical treatment [8], photo catalysis [9] and biological treatment [10]. But these treatment methods pose technological or economical limitations. Adsorption technique is the most versatile, cost-effective and widely used method for wastewater treatment. The most common adsorbent materials are silica [11] and activated carbon [12]. Studies have shown that the above-said adsorbents for the adsorption of different types of dyes are efficient, but their use is restricted due to their higher cost. It has resulted in finding alternative low-cost adsorbents [13], which may replace the conventional adsorbents in pollution control. Low-cost alternative adsorbents are natural materials or the wastes or by-products of industries [13].

Waste natural materials such as hen feather [14–16], egg shell waste [17,18], egg shell membranes [19] and industrial wastes such as nanoalumina [20] and bottom ash [21] have been used for the removal of dyes, heavy metals and organic pollutants from wastewater.

Red mud is the insoluble solid waste remaining after the caustic digestion of bauxite used for production of alumina by the Bayer process. Red mud causes serious environmental pollution-related problems due to its high alkalinity and production in large amount as a solid waste. Environmental concerns have led to extensive research to find effective ways to utilize the abundantly available red mud from aluminium industry. Red mud has been studied as one of the low-cost unconventional adsorbent, for the removal of fluoride [22], heavy metals [23–25] and dyes from aqueous solution. Several studies have reported that red mud can be utilized for adsorbing dyes such as Congo red [26], Rhodamine B, Fast Green, and Methylene Blue [27]. Red mud activated with dilute sulphuric acid was found to be a very efficient adsorbent for removal of RBB, a reactive dye [28]. Activation by dilute sulphuric acid was found to improve the adsorption. Search for better activation method to enhance the adsorption is necessary for the removal of high concentrations of the dye from contaminated wastewaters. Thus, this study attempts to use concentrated sulphuric acid treatment for activation of red mud to enhance the adsorption capacity of red mud for the removal of RBB from contaminated water. Reuse of industrial solid waste for the treatment of wastewater from another industry will help not only in solving the solid waste disposal problem, but also in reducing the treatment cost of wastewater.

This study presents the removal of RBB by adsorption using red mud treated with concentrated H_2SO_4. Industrial-scale application of the process necessitates the optimization of parameters affecting the adsorption process. Number of experiments, time and overall research cost may be reduced by employing "Design of experiments" strategy for optimization. "One factor at a time" method is often insufficient to account for interaction between the factors affecting the process performance. Several researchers have used "Design of experiments" for modelling and optimization of adsorption process for removal of heavy metals and dyes using different adsorbents [29–31]. Thus, in this study experiments were designed based on central composite design (CCD) and response surface methodology (RSM) was used for optimization of the adsorption process.

2. Materials and methods

2.1. Red mud and dye

Red mud (composition: Fe_2O_3 (42%), Al_2O_3 (20%), TiO_2 (9%), SiO_2 (10–12%), Na_2O (4–5%)) was obtained from Hindalco Aluminium Industry, Belgaum, India. RBB dye (90% pure) was gifted by Campbell Knitwear Ltd, Belgaum, India. The dye concentration was estimated by measuring the absorbance at 608 nm (λ_{Max}) using a precalibrated UV–vis bio-spectrophotometer (Elico BL-198).

2.2. Pretreatment and characterization of raw red mud

Red mud was washed thoroughly with distilled water, filtered and dried at 110˚C for 24 h. 10 g of this red mud was soaked in 20 ml concentrated H_2SO_4 (98%) for 4 h. Then, the red mud was separated from the digestion slurry by filtration, washed with distilled water several times and dried in an oven at 110˚C overnight. This formed the concentrated acid-treated red mud (CATRM).

Characterization of raw red mud and CATRM samples were carried out by X-ray diffraction (XRD) and scanning electronic microscopy (SEM) for surface morphology and composition to compare the relative performance of raw red mud and CATRM. The X-ray diffractograms of these samples were obtained using JEOL X-ray diffractometer, using CuK-alpha radiation ($\lambda = 1.5425$ Å, $V = 40$ kV, $I = 20$ mA). The SEM analysis and energy-dispersive X-ray (EDAX) of the samples were carried out by JED 2300 Analysis JEOL. The surface area of raw red mud and CATRM were determined by BET analysis using ASAP 2020 V3.04 H, Micromeritics, USA. The chemical composition of raw red mud and CATRM was determined by X-ray fluorescence (XRF) spectroscopy, using Philips PW2400 XRF spectrometer.

2.3. Batch adsorption experiments

Batch adsorption experiments were carried out in 100-ml conical flasks containing the aqueous dye solution of known concentration and with CATRM at desired quantity. Initial pH of the solution was adjusted to the desired value with 1 N NaOH or 1 N HCl solutions. The solution was agitated with a constant speed of 145 rpm in an incubator-shaker maintained at a required temperature till the equilibrium condition was reached. The solution containing red mud was then centrifuged to separate the supernatant from red mud. The solution was centrifuged at 4,000 rpm in Remi centrifuge to separate the adsorbent from the solution. The equilibrium dye concentration of supernatant was determined using UV spectrophotometer. Batch adsorption experiments were performed at different initial dye concentrations in the range of 50–150 mg/l, CATRM dosages in the range of 0.3–1.8 g/l, temperature 20–40˚C range and pH varying from 2 to 12.

2.4. Design of experiments for optimization of parameters

To aid in the optimization of parameters such as pH, initial dye concentration, CATRM dosage and temperature for efficient removal of the dye, batch experiments were designed as per CCD with four factors at five levels. The range of levels in coded and uncoded form for different factors are presented in Table 1.

The response variable in this study is the percentage adsorption of dye at equilibrium. Thirty-one sets of batch adsorption shake flask experiments were carried out as per CCD under conditions shown in Table 2.

2.5. Analysis and optimization

The results of the batch experiments based on CCD set were subjected to analysis using RSM. The effect of four factors (initial pH, CATRM dosage, initial dye concentration and temperature) as individuals and in combination as interacting effect on the response (% adsorption of the dye) was evaluated using RSM. Multiple regression analysis (MRA) on the experimental input–output data was performed using MINITAB 14 software. The results were fitted into the regression equation, and the effects of factors on the response were analysed by RSM. The analysis included the linear and quadratic effects of the four factors and their interactions. Thus, the equation giving percentage dye adsorption (response), as a function of the factors, is presented as Eq. (1) a second-order polynomial model with 15 coefficients (b_0, b_1, $b_{12} \ldots b_{34}$).

$$Y = b_0 + b_1X_1 + b_2X_2 + b_3X_3 + b_4X_4 + b_{11}X_1^2 + b_{22}X_2^2 + b_{33}X_3^2 + b_{44}X_4^4 + b_{12}X_1X_2 + b_{13}X_1X_3 + b_{14}X_1X_4 + b_{23}X_2X_3 + b_{24}X_2X_4 + b_{34}X_3X_4 \quad (1)$$

where X_1, X_2, X_3 and X_4 are the uncoded factors studied and Y is the response.

The significance of the terms in the model was evaluated using analysis of variance (ANOVA) based upon the F-test with unequal variance ($p < 0.05$). Statistically significant model correlating the percentage adsorption of the dye with the input variables was hence developed. The optimum values of initial pH,

Table 1
Factors and levels (coded and uncoded) used in the central composite design

Factors	−2	−1	0	+1	+2
pH(X_1)	1	2	3	4	5
Initial concentration(X_2), mg/l	50	75	100	125	150
Red mud dosage (X_3), g/l	0.3	0.75	1.2	1.65	2.1
Temperature(X_4), ˚C	20	25	30	35	40

Table 2
Batch adsorption experiments as per CCD

Run no	pH	Initial concentration, mg/l	Dosage, g/l	Temperature, ℃
1	2	75	1.65	25
2	4	125	0.75	25
3	3	100	2.1	30
4	3	100	1.2	40
5	2	75	0.75	25
6	4	75	1.65	25
7	1	100	1.2	30
8	4	75	0.75	35
9	3	100	1.2	30
10	3	50	1.2	30
11	3	100	1.2	30
12	3	100	1.2	30
13	4	125	1.65	35
14	2	75	0.75	35
15	3	150	1.2	30
16	2	75	1.65	35
17	3	100	1.2	20
18	3	100	1.2	30
19	4	75	1.65	35
20	3	100	1.2	30
21	2	125	1.65	35
22	2	125	0.75	25
23	2	125	1.65	25
24	4	125	1.65	25
25	5	100	1.2	30
26	4	75	0.75	25
27	2	125	0.75	35
28	4	125	0.75	35
29	3	100	1.2	30
30	3	100	1.2	30
31	3	100	0.3	30

red mud dosage, initial dye concentration and temperature were obtained using response optimizer of MINITAB 14. Response surface plots were generated using these input–output data.

3. Results and discussions

3.1. Red mud characterization

Raw red mud is a complex mixture of phases comprising of haematite (Fe_2O_3), goethite (FeOOH), gibbasite ($Al(OH)_3$), anatase (TiO_2) and quartz (SiO_2). The XRD of raw red mud and CATRM samples were obtained. From XRD pattern, after the acid treatment, the intensity for haematite (104) and goethite (240) increased, and the peaks for haematite (024) and goethite (002) had almost disappeared, suggesting the phase transformation of red mud during activation. The surface of the red mud activated by acid pretreatment was compared with that of raw red mud using the results of SEM. SEM-EDAX analysis showed that the intensity for metals such as Al, Si, Ti and Fe in raw red mud was very high. The intensities of elements such as Al, Si, Ti and Fe in raw red mud were 60, 25, 10 and 15, respectively. Drastic decrease in intensities of Fe, Ti, Si and Al was observed after the acid treatment. Similar results were obtained by Agatzini-Leonardou et al. [32]. The acid treatment leads to dispersion of dissolved metal oxides as hydroxides which leads to formation of pores. On acid treatment, the adsorbed salts and exchangeable cations are dissolved first, and then, aluminium ions and other metallic ions are removed from the lattice of structure so that many micropores are created [33]. Decreased metal intensities on acid treatment confirms the removal of cations from the surface.

BET analysis showed that the raw red mud and CATRM have specific surface area of 20.2 and

32.28 m^2/g, respectively. Table 3 presents the surface area, pore volume and pore size of raw and CATRM. Concentrated acid treatment has increased the surface area, pore volume and decreased the pore size. Surface area of the dilute acid-treated red mud was reported to be 27.30 m^2/g [28]. Surface area of CATRM is higher than that obtained with dilute acid-treated red mud. Significant improvement in surface characteristics could be attained by concentrated acid treatment.

Table 4 shows the chemical composition of the raw red mud and CATRM as obtained using XRF spectroscopy. It shows that CATRM has greater silica content and lower abundance of other metal oxides. The Si^{4+}cations at tetrahedral sites of red mud would not have dissolved by acid activation. Similar observations were made by Regina and Ajemba [34] in their studies on acid-treated Udi clay. The increased surface area of CATRM as compared to raw red mud may be attributed to the removal of impurities, replacement of exchangeable cations (Na^+ and Ca^+) with hydrogen ions and leaching of Al^{+3}, Mg^{+2} and Fe^{+3} from octahedral and tetrahedral sites [34] which expose the edges of the red mud sample. Sulphuric acid treatment has also led to the increase of SO_3 concentration in CATRM.

3.2. Effect of pH

The pH of the dye solution plays an important role in the whole adsorption process and particularly on the adsorption capacity. The adsorption of charged dye groups onto the CATRM surface is primarily influenced by the surface charge on the adsorbent, which in turn is influenced by the initial pH of the solution. The batch adsorption experiments were conducted at different initial pH ranging from 2 to 12. Fig. 1 shows the effect of initial pH on percentage removal of dye at equilibrium, with initial dye concentration of 50 mg/l and CATRM dosage of 1.2 g/l. The percentage removal of dye by adsorption has decreased with the increase in pH from 2 to 12. At a pH range between 4 and 8, a considerable decrease in adsorption takes place. The percentage removal decreased with increase in pH. This variation is quite similar to the previous reports [35] for removal of Acid Violet using red mud. The decrease in removal of dye with increase in pH may be explained on the basis of acid–base dissociation at solid/liquid interface [35]. As highly acidic conditions showed better adsorption, to design the experiments as per CCD for optimization studies, pH range of 1–5 was selected.

3.3. Effect of contact time

The effect of contact time on percentage adsorption of RBB on CATRM, at different initial RBB concentrations, is shown in Fig. 2. It can be observed that the adsorption is faster for 60 min of initial time, but the adsorption took place at a lower rate for the

Table 3
Characterization of raw red mud and red mud treated with concentrated sulphuric acid

Sample	Surface area, m^2/g	Pore volume, cm^3/g	Pore size, nm
Raw red mud	20.2	0.093	20.98
CATRM	32.28	0.119	19.21

Table 4
Chemical composition of raw red mud and acid-treated red mud

Oxides	Raw red mud (composition, %)	CATRM (composition, %)
Fe_2O_3	36.16	24.71
Al_2O_3	24.30	13.87
SiO_2	13.59	22.30
Na_2O	11.28	0.12
TiO_2	10.29	14.29
CaO	2.40	0.08
P_2O_5	0.42	0.23
SO_3	0.41	2.36
MgO	0.24	0.13

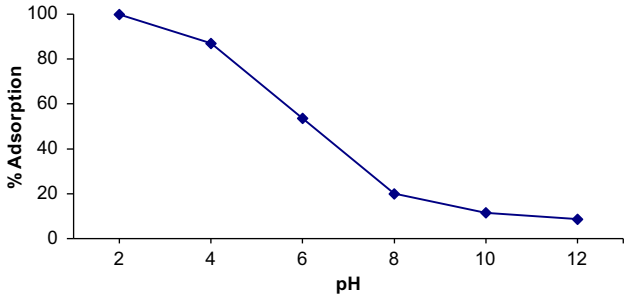

Fig. 1. Effect of initial pH on percentage adsorption of dye. Conditions: initial dye concentration = 50 mg/l, temperature = 30°C and CATRM dosage = 1.2 g/l.

remaining time. The amount of adsorbed RBB increased with contact time and then attained a constant value at 300 min. This trend was observed at all the initial RBB concentrations studied. Similar results were observed by Tor and Cengeloglu [26], during the removal of Congo red by red mud. As at the initial time, the dye solution concentration is higher, the driving force is the maximum, leading to maximum rates. But as the adsorption proceeds, the bulk concentration reduces approaching the equilibrium value and the rate decreases [28]. The time to reach equilibrium condition is around 300 min for all the initial dye concentrations studied. Thus, 300 min was found to be sufficient for the attainment of equilibrium in the prevailing shaking conditions of 145 rpm.

3.4. Effect of adsorbent dosage

The removal of dye with varying amount of red mud was studied for different initial dye concentrations. Results of this study are shown in Fig. 3. The adsorption of dye has increased with increase in CATRM dosage. The percentage adsorption of dye increased by 5% when the quantity of CATRM used was doubled from 0.3 to 0.6 g/l. As the amount of CATRM was increased further to 1.2 g/l, the dye removal had increased by only around 2%. It can be observed from Fig. 3 that there is only a negligible change in percentage adsorption when the CATRAM dosage increased from 1.5 to 1.8 g/l, at all the initial dye concentrations studied. Thus, 1.5 g/l of adsorbent was considered to be quite appropriate, as further increase in dosage did not show much increase in uptake of dye.

The increase in the amount of dye removal with adsorbent dosage is due to greater availability of active sites. Fig. 4 shows the sample plot of the effect of adsorbent dosage on dye adsorption capacity, for dye solution with initial concentration of 130 mg/l. It can be seen from Fig. 4 that the adsorption capacity decreased with an increase in the adsorbent dosage, though the percentage adsorption had increased with the increase in adsorbent dosage as shown in Fig. 3. Similar trends were also observed with other initial dye concentrations. This suggests that as the number of particles increases, there may be over crowding of the adsorbent particles in solution, which may lead to overlapping of adsorption sites or adsorbed species causing the particles to aggregate, thereby resulting in reduced adsorption active sites per unit mass of the adsorbent [36]. At high adsorbent dosage, due to larger probability of collision between the adsorbent particles, the particles tend to aggregate, and hence, the adsorption capacity decreases.

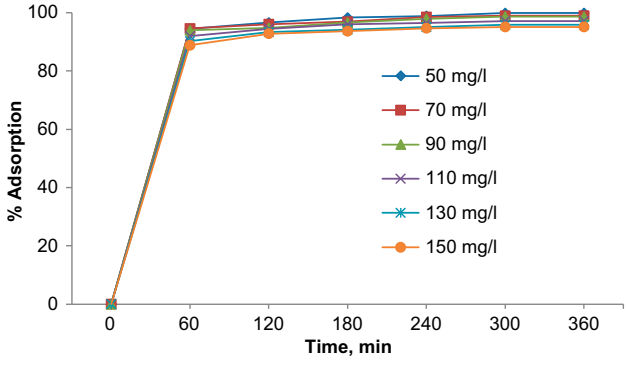

Fig. 2. Effect of contact time on percentage adsorption of dye at different initial dye concentration. Conditions: pH 2; temperature = 30°C and CATRM dosage =1.2 g/l.

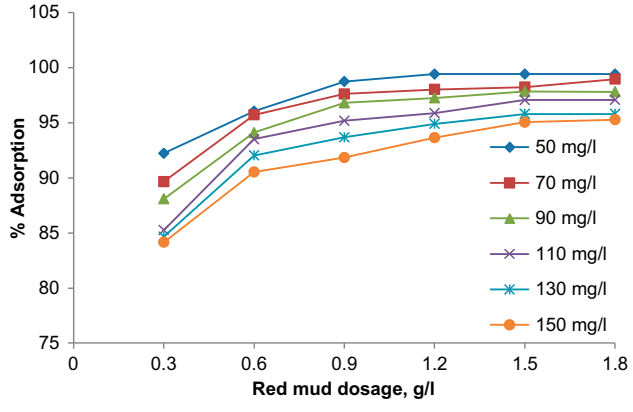

Fig. 3. Effect of CATRM dosage on percentage adsorption. Conditions: pH 2 and temperature = 30°C.

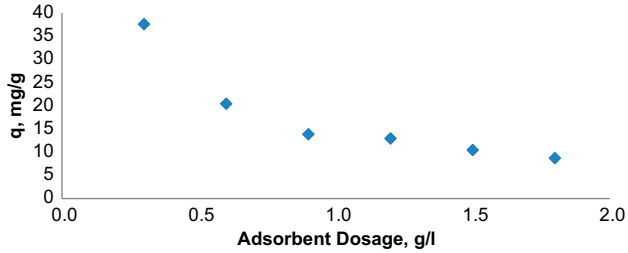

Fig. 4. Effect of CATRM dosage on adsorption capacity. Conditions: pH 2, initial concentration of dye = 130 mg/l and temperature = 30°C.

3.5. Adsorption isotherm

The relationship between the amount of dye adsorbed and the equilibrium dye concentration remaining in solution is described by adsorption isotherms. The two most common isotherms which define adsorption equilibrium are Langmuir and Freundlich isotherms.

The most important model of monolayer adsorption is the Langmuir isotherm; the linear form of which is shown in Eq. (2).

$$\frac{C_e}{q_e} = \frac{1}{Q_o b} + \frac{1}{C_e Q_o} \tag{2}$$

where C_e is the dye solution concentration of RBB (mg/l) at equilibrium, q_e is the amount of adsorbed dye per unit mass of adsorbent (mg/g), Q_o the monolayer capacity of the adsorbent (mg/g), and b is the Langmuir adsorption constant indicating the adsorption energy (l/mg).

The Freundlich isotherm is an empirical model applied to model the multilayer adsorption system and for the adsorption on heterogeneous surfaces. The linear form of Freundlich model is given as in Eq. (3).

$$\ln q_e = \ln k + \frac{\ln C_e}{n} \tag{3}$$

where k is the sorption capacity (mg/g) and n is an empirical parameter which is an indicator of adsorption intensity. The equilibrium data obtained from the experiments were fitted into these two types of isotherms to test the validity of these for RBB-CATRM adsorption system. The values of parameters of the isotherms at three different temperatures of 20, 30 and 40°C, along with the corresponding R^2 values are presented in Table 5.

The R^2 values indicate that the equilibrium for RBB-CATRM adsorption system can be represented by both Langmuir and Freundlich isotherms under the conditions of the study. Significant fit into both the models may be owing to lower dye concentrations employed in the study, under circumstances in which both the models may be applicable. But Langmuir isotherm is found to fit the data better at all the studied temperatures as depicted by higher R^2 values. From the results of Langmuir isotherm parameters, it is clear that the values of monolayer capacity Q_o and adsorption energy b of CATRM increase with the increase in temperature. It is known that smaller the value of n ($1 < n < 10$), higher is the adsorption intensity [37,38]. Similarly greater the k value, higher is the adsorption capacity of the adsorbent for the dye molecule. Hence, increase in k and n of Freundlich model with increasing temperature suggests that adsorption capacity of CATRM for RBB is higher at higher temperatures. Thus, it may be concluded that high temperature favours the adsorption.

The essential characteristics of the Langmuir isotherm can be expressed by a separation or equilibrium parameter (R_L), which is given by Eq. (4).

$$R_L = \frac{1}{(1 + bC_0)} \tag{4}$$

where C_0 is the initial concentration of dye (mg/l) and b is the Langmuir constant (l/mg). R_L indicates the nature of the adsorption process as given below:

$R_L > 1$ Unfavourable
$R_L = 1$ Linear
$0 < R_L < 1$ Favourable
$R_L = 0$ Irreversible

The values of R_L were found to be in the range of 0–1 as shown in Table 6, indicating that the process of adsorption of RBB on CATRM is favourable. The R_L values obtained with dilute sulphuric

Table 5
Adsorption isotherm parameters at different temperature

Temperature, °C	Langmuir model	Freundlich Model
20	$Q_o = 100$ mg/g $b = 0.16$ l/mg $R^2 = 0.991$	$n = 1.29$ $k = 19.16$ mg/g $R^2 = 0.978$
30	$Q_o = 111$ mg/g $b = 2.25$ l/mg $R^2 = 0.980$	$n = 2.84$, $k = 58.18$ mg/g $R^2 = 0.989$
40	$Q_o = 125$ mg/g $b = 8$ l/mg $R^2 = 0.984$	$n = 3.11$ $k = 87.35$ mg/g $R^2 = 0.939$

Table 6
R_L values at different initial concentrations at 30°C

C_0, mg/l	R_L
50	0.009
70	0.007
100	0.004
110	0.004
130	0.003
150	0.003

acid-treated red mud with different initial concentrations are around 0.10 [28]. The R_L for CATRM are much lesser than one, indicating that adsorption of dye on red mud treated with concentrated sulphuric acid is highly favourable than that treated with dilute acid.

3.6. Process optimization by RSM

Thirty-one sets of experiments, shown in Table 7, designed as per CCD matrix, were conducted to study the effect of different factors influencing the adsorption process as an individual and on interaction with each other, as well as with a view to optimize the process using RSM. The matrix of four variables pH (X_1), initial concentration of dye (X_2), adsorbent dosage (X_3) and temperature (X_4) were varied at five levels (−2, −1, 0, +1, +2). The higher level of variable was designated as "+", and the lower level was designated as "−". Dye removal percentage obtained from the experiments at the end of 300 min (equilibrium time) for each of the experiments are shown in Table 7.

MRA of the experimental data was performed based on ANOVA using RSM with MINITAB 14. Multiple regression model relating the factors in uncoded form to the response were developed with the regression coefficients. The MRA model developed in terms of uncoded factors is shown in Eq. (5).

$$\begin{aligned}\%\ \text{Adsorption} = {} & 123.7 - 12.39X_1 - 0.162X_2 + 0.56X_3 \\ & + 1.284X_4 + 1.709X_1^2 + 0.001X_2^2 \\ & - 2.69X_3^2 + 0.023X_4^2 + 0.011X_1X_2 \\ & + 0.33X_1X_3 + 0.0050X_1X_4 \\ & - 0.0362X_2X_3 - 0.002X_2X_4 \\ & + 0.489X_4X_3\end{aligned} \tag{5a}$$

The MRA model developed in terms of coded factors is shown in Eq. (5b).

Table 7
Experimental design matrix and results for the dye removal percentage

Run no	Predicted % removal	Experimental % removal
1	85.65	85
2	69.65	70
3	81.35	80
4	85.18	85
5	81.83	80
6	76.83	78
7	90.85	93
8	75.66	75
9	78	78
10	84.45	86
11	78	78
12	78	78
13	79.05	80
14	84.99	85
15	75.18	72
16	93.23	92
17	75.45	74
18	78	78
19	84.49	85
20	78	78
21	86.69	88
22	77.99	80
23	80.22	80
24	72.49	75
25	73.78	70
26	72.39	74
27	80.05	78
28	71.83	75
29	78	78
30	78	78
31	70.28	70

$$\begin{aligned}\%\ \text{Adsorption} = {} & 68.216 - 9.25X_1 - 2.71X_2 + 1.077X_3 \\ & + 0.413X_4 + 4.316X_1^2 + 1.816X_2^2 \\ & - 0.0218X_3^2 + 2.3167X_4^2 + 1.1X_1X_2 \\ & + 0.06X_1X_3 + 0.1X_1X_4 - 0.16X_2X_3 \\ & - 1.1X_2X_4 + 0.44X_4X_3\end{aligned} \tag{5b}$$

Eq. (5a) can be used for prediction of % adsorption at the required values of the factors. The coefficients of terms in Eq. (5b) explain the relative significance of the terms on the percentage adsorption. The coefficients of X_1 (pH) and X_2 (initial concentration) are negative terms indicating that with increase in these parameters, the percentage removal of dye decreases. The positive coefficients of X_3 (dosage) and X_4 (temperature) indicate that the percentage removal

increases with increase in these parameters. On comparison of coefficients of X_1, X_2, X_3 and X_4 in Eq. (5b), and as observed from high value of the coefficient for X_1, the effect of pH is highly significant, followed by initial concentration and then dosage and temperature. These results are concurrent with one factor at a time experimental results described earlier. Though X_1 and X_2 individually showed negative effect, the interaction effect was positive as indicated by the positive coefficient of X_1X_2 term. Similarly, though X_1 and X_3; X_1 and X_4 had opposing effects, the net interaction effects were positive, indicating that pH and dosage effects interact with each other to increase the adsorption. Similarly, pH and temperature effects interact with each other to increase the adsorption. However, dosage effect in interaction with the initial dye concentration effect provides negative effect on adsorption, though individually, dosage has a positive effect. The positive effect of dosage is masked by the negative effect of initial dye concentration, thus providing overall negative effect.

Similarly, the positive effect of temperature is masked by the negative effect of initial concentration, providing an overall negative effect on the interaction of these factors. However, dosage and temperature effects are positive individually as well as on interaction with each other. But as observed from the coefficients of X_3, X_4 and X_4X_3, it can be concluded that their individual positive effects are higher, but the interaction effect is lower as compared to the individual effects. As observed from the coefficients of product terms, the interaction effects between pH–initial concentration and initial concentration–temperature are the maximum, followed by that of dosage and temperature. The interaction effects between pH–temperature and initial concentration–dosage are not very significant. pH and dosage showed least interaction effect, as observed from the least value of coefficients among the product terms.

ANOVA showed that the main and interaction terms are highly significant ($P < 0.05$) and that the model is well applicable. The coefficient of determination ($R^2 = 0.94$) for the model was high, showing good fit of the statistical model. Predicted values of percentage removal for all the 31 experiments are shown in Table 6 and are found to agree well with the experimental values. ANOVA indicated that the second-order polynomial model Eq. (5) is highly significant and adequate to represent the actual relationship between the response (percentage removal efficiency) and the variables, with P-value of 0.006 and a high value of coefficient of determination.

Process optimization was carried out based on the data using "Response optimizer" tool of MINITAB 14. The optimum values found were the following: pH 1.00, initial dye concentration = 105 mg/L, CATRM dosage = 2.05 g/l and temperature = 31.65°C. The batch experiments were conducted at these optimum conditions, and it was found that 99% adsorption of the dye occurred in 300 min, showing the significance of optimization strategy. The predicted value of percentage adsorption from the model under these conditions was 99.9%. The predicted value of percentage adsorption from the model under optimum conditions matches well with the experimental value, with negligible error. It indicates the validity of the model. As optimum CATRM dosage is a function of dye concentration, it is more appropriate to represent the optimum dye to CATRM dosage ratio than the optimum CATRM dosage. The optimum dye to adsorbent (CATRM) dosage ratio was 0.051 g/g.

The combined effect of initial pH and temperature on adsorption of dye at constant dosage (2.05 g/l) and initial concentration (105 mg/l) is shown in the surface

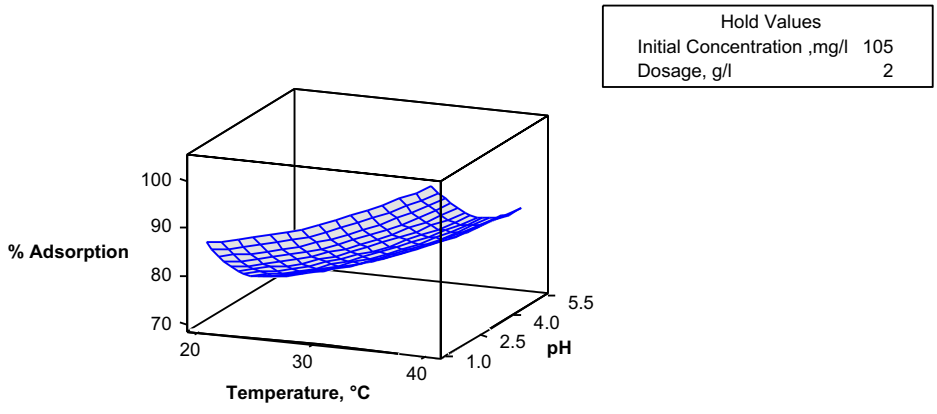

Fig. 5. Surface plot for effect of pH and temperature on % adsorption.

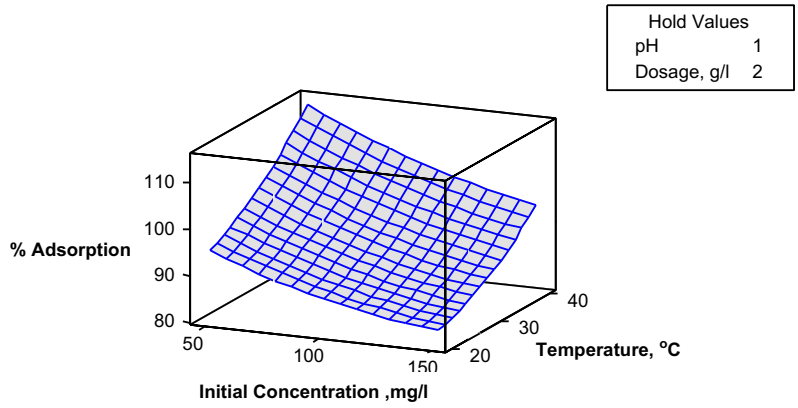

Fig. 6. Surface plot for effect of initial concentration and temperature on % adsorption.

plot presented as Fig. 5. It can be seen that with increase in pH value, the percentage adsorption of the dye decreases in the entire temperature range studies. The percentage adsorption is higher at low pH and higher temperature. The effect of temperature on percentage adsorption seems nearly similar in the entire range of pH studied, indicating marginal interaction between these variables.

Fig. 6 shows the interaction effect of temperature and initial concentration of dye on percentage adsorption of dye onto CATRM at constant dosage of 2.05 g/l and pH of 1. It shows that as the initial concentration of dye increases, the percentage adsorption decreases. Increase in temperature leads to increase in percentage adsorption. Percentage adsorption is highly favoured at higher temperatures and lower initial dye concentrations. However, the effect in temperature on percentage adsorption seems to be significant at lower concentration condition as compared to that at higher concentration, indicating the interaction effect.

The three-dimensional response surface for the combined effect of initial concentration of dye and dosage on adsorption of dye at constant pH (1) and temperature (31.65˚C) is shown in Fig. 7. Percentage adsorption decreases with the increase in initial dye concentration and increases with increase in adsorbent dosage. With higher dosage and lower concentrations, the maximum removal of dye can be observed. Effect of adsorbent dosage appears to be nearly similar in the entire initial dye concentration range, indicating marginal interaction effect between these factors.

The combined effect of pH and adsorbent dosage on adsorption of dye at constant temperature (31.65˚C) and initial concentration of dye (105 mg/l) is shown in Fig. 8. Percentage adsorption decreases with increase in pH. The percentage adsorption increases with the increase in adsorbent dosage. Minimum adsorption was found to be at a pH of around 5.5 and at lowest adsorbent dosage. The effect of dosage on percentage adsorption is similar in the entire range of pH. Hence, dosage and pH interaction is marginal.

Fig. 9 shows the three-dimensional response surface which was constructed to show the effect of temperature and adsorbent dosage on the adsorption of dye at constant pH of 1 and initial dye concentration of 105 mg/l. It can be observed from Fig. 9 that the percentage removal increases with the increase in adsorbent dosage. Percentage removal increases significantly with the increase in temperature. But, at lower values of temperature, the percentage adsorption increases with dosage, up to a certain value, and then remains almost constant with further increase of dosage. However, as the temperature increases percentage adsorption increases sharply with the increase in dosage. Very sharp increase in percentage adsorption with dosage is observed in Fig. 9, at the highest temperature of 40˚C. Thus, the interaction effect between the dosage and temperature is significant.

Fig. 10 shows the three-dimensional response surface to explain the combined effect of pH and initial concentration on adsorption of dye at constant dosage (2.05 g/l) and temperature (31.65˚C). The percentage adsorption is more in lower concentration region and at lower pH values. But the percentage adsorption decreases with higher concentration and with higher pH values. The effect of pH is very pronounced at lower initial concentration range. But the effect of pH seems to be minimal at high initial concentration. This indicates that the interaction effect between the pH and initial concentration is highly significant.

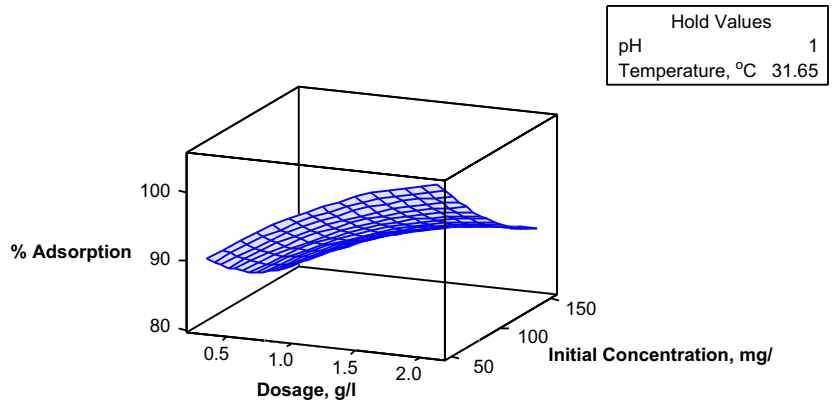

Fig. 7. Surface plot for effect of initial concentration and dosage on % adsorption.

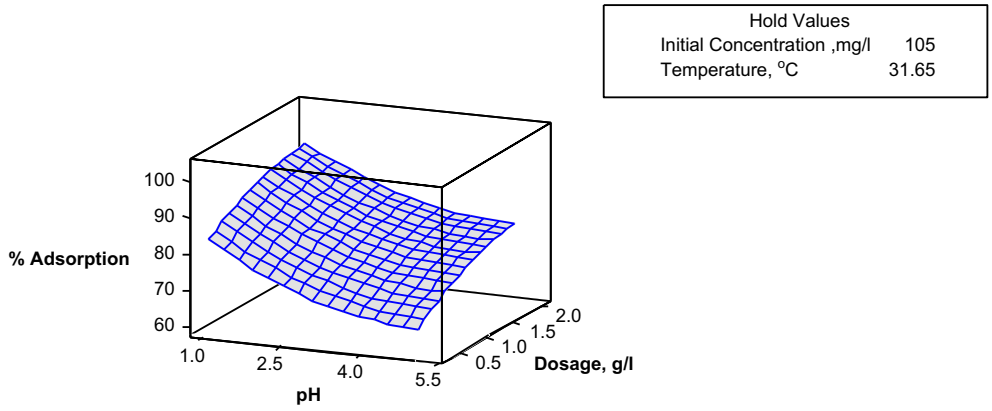

Fig. 8. Surface plot for effect of pH and dosage on % adsorption.

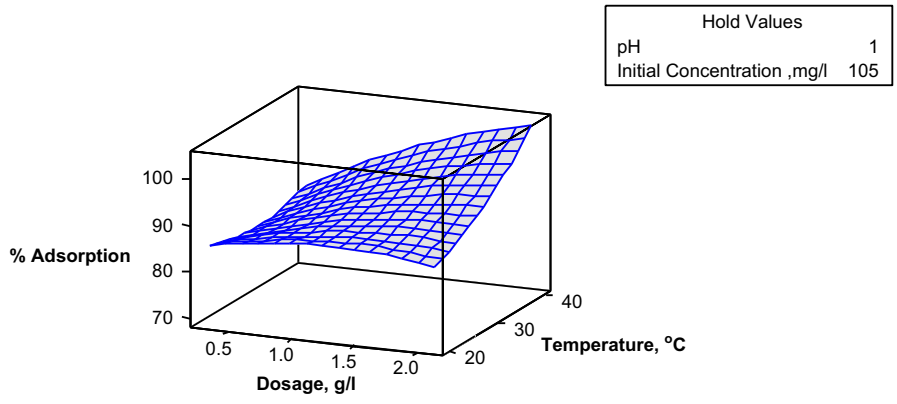

Fig. 9. Surface plot for effect of dosage and temperature on % adsorption.

3.7. Effect of dye to adsorbent dosage ratio on percentage adsorption for CATRM

Amount of adsorbent needed to provide enough adsorption sites for given amount of dye is a very crucial parameter in adsorption. Dye to adsorbent ratio to provide just enough adsorption sites should be a constant value. This value is very important in designing continuous adsorption systems for

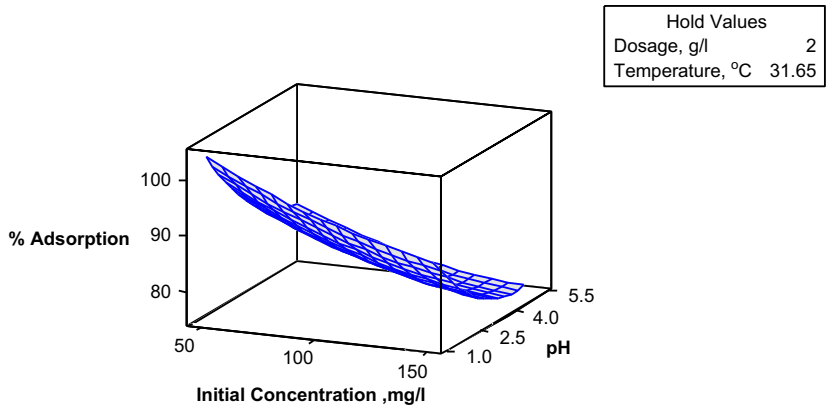

Fig. 10. Surface plot for effect of pH and initial concentration on % adsorption.

industrial-scale operation. From the optimum values of dye concentration and dosage obtained by optimization, the optimum ratio of dye to adsorbent dosage was obtained. The required adsorbent dosage varies with the dye concentration. To study the effect of initial dye concentration on adsorption with a constant dye to adsorbent ratio, experiments were performed by varying the amount of CATRM dosage and the initial concentration of dye independently, so that the initial dye to adsorbent dosage ratio was kept constant at the optimum value of 0.051 g dye/g of adsorbent. Batch studies were carried out at optimum conditions of pH 1 and temperature = 31.65°C. Experiments were carried out with initial dye concentration of 50–130 mg/l. Adsorbent dosages were varied so that dye to dosage ratio was kept constant at 0.051 g dye/g CATRM. Time course variations of percentage adsorption at different combinations of both initial dye concentrations and red mud dosage with constant dye to dosage ratio (g/g) are as shown in Fig. 11.

The percentage adsorption reached a maximum of 100% within 300 min contact time with all the initial dye concentrations. But for lower concentration of 50 mg/l, 100% adsorption was reached faster than that with higher concentration. The adsorption rate is fast for lower concentrations of dye as compared to that at higher concentrations. The results showed that at constant value of dye to dosage ratio, the maximum percentage adsorption does not depend upon the initial dye concentration, whereas the rate of adsorption varies with the initial dye concentration.

3.8. Adsorption kinetics

In order to, evaluate the adsorption kinetics, available kinetic models were tested with the batch data. The batch experimental data under optimum conditions (pH 1, temperature 31.65°C and dye to dosage ratio 0.051 g/g) with initial dye concentration of 105 mg/l were analysed using the pseudo-first-order and pseudo-second-order adsorption kinetic models, and kinetic constants were calculated. The rate constants of the adsorption process carried out at initial concentration of 105 mg/l for fixed temperature of 31.65°C were determined.

The linear form of pseudo-first-order rate equation is given by the Eq. (6).

$$\log(q_e - q) = \log(q_e) - \left(\frac{K_1}{2.303}\right)t \tag{6}$$

where q is the amount of adsorbate adsorbed at time t (mg/g), q_e is the adsorption capacity at equilibrium (mg/g), and K_1 is the pseudo-first-order rate constant. The value of pseudo-first-order rate constant was found to be 0.016 (min^{-1}) with coefficient of determination (R^2) value of 0.84. The model's predicted

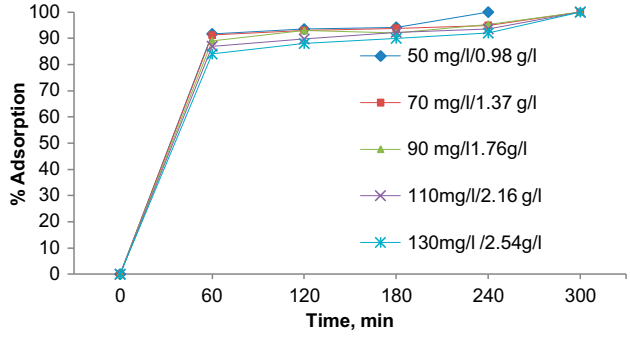

Fig. 11. Effect of initial dye concentration and CATRM dosage on % adsorption at constant dye to dosage ratio (0.051). Conditions: pH 1 and temperature = 31.65°C.

(24.26 mg/g) value of q_e largely deviated from the experimental value (73.16 mg/g). Thus, pseudo-first-order kinetic model is not the valid model to represent the adsorption kinetics of RBB on CATRM. Thus, pseudo-second-order kinetic equation which is also based on the sorption capacity of the solid phase was tested. The linear form of pseudo-second-order kinetic equation is given by the Eq. (7).

$$\frac{t}{q} = \frac{1}{q_e^2 K_2} + \frac{t}{q_e} \tag{7}$$

where K_2 is the rate constant of pseudo-second-order adsorption kinetic equation (g/mg min). The pseudo-second-order rate constant was obtained from the slope and intercept of the plot of $\frac{t}{q}$ against t. Pseudo-second-order kinetic model with the R^2 value of 0.99 has been found to fit the data better than the first-order kinetics model. The experimental and the predicted values of q_e from the pseudo-second-order kinetic model match well with very minimal error. These results suggest that sorption kinetics follows the pseudo-second-order model with kinetic rate constant of 0.0063 g/mg/min.

4. Conclusion

The adsorption of RBB dye using red mud treated with concentrated sulphuric acid was studied. The concentrated acid treatment was found to increase the surface area of red mud by 12 m^2/g. Highly acidic conditions were found to favour the adsorption process. Around 100% removal of 50 mg/l RBB and 97% removal for 150 mg/l of RBB could be attained with the CATRM dosage of 1.5 g/l. Langmuir isotherm model has been found to represent the equilibrium data for RBB-CATRM adsorption system better than Freundlich model. Factors affecting adsorption process were optimized using RSM, based on the experiments designed as per CCD. The optimum conditions for maximum removal of RBB on CATRM were pH 1, initial dye concentration = 105 mg/l, red mud dosage = 2.05 g/l and temperature = 31.65°C. Optimum ratio of dye to CATRM dosage was found to be 0.051 g/g. At constant values of dye to dosage ratio, the maximum percentage adsorption does not depend upon the initial dye concentration, whereas the rate of adsorption varies with the initial dye concentration. The sorption kinetics for CATRM-RBB adsorption system follows the pseudo-second-order model with kinetic rate constant of 0.0063 g/mg/min. The process of adsorption of dyes using red mud involves the reuse of red mud, a waste product from alumina industry for the treatment of wastewater from other industries such as textiles and hence will not only help in solving the solid waste disposal problem, but also reduces the treatment cost of wastewater.

References

[1] O. Gulnaz, A. Kaya, F. Matyar, B. Arikan, Sorption of basic dyes from aqueous solution by activated sludge, J. Hazard. Mater. 108 (2004) 183–188.
[2] A.S. Mahmoud, A.E. Ghaly, S.L. Brooks, Influence of temperature and pH on the stability and colorimetric measurement of textile dyes, Am. J. Biochem. Biotechnol. 3 (2007) 33–34.
[3] K. Hunger (Ed.), Industrial Dyes: Chemistry, Properties, Applications, Wiley-VCH, Weinheim, 2003.
[4] D. Suteu, C. Zaharia, D. Bilba, A. Muresan, R. Muresan, A. Popescu, Decolorization waste waters from the textile industry—Physical methods, chemical methods, Ind. Text. 60(5) (2009) 254–263.
[5] D. Suteu, C. Zaharia, A. Muresan, R. Muresan, A. Popescu, Using of industrial waste materials for textile wastewater treatment, Environ. Eng. Manage. J. 8(5) (2009) 1097–1102.
[6] N. Mathur, P. Bhatnagar, P. Bakre, Assessing mutagenicity of textile dyes from Pali (Rajasthan) using amesbioassay, Appl. Ecol. Environ. Res. 4 (2005) 111–118.
[7] P.K. Malik, S.K. Saha, Oxidation of direct dyes with hydrogen peroxide using ferrous ion as catalyst, Sep. Purif. Technol. 31 (2003) 241–250.
[8] S.H. Lin, C.F. Peng, Treatment of textile wastewater by electrochemical method, Water Res. 28 (1994) 277–282.
[9] A. Aguedach, S. Brosillon, J. Morvan, E.K. Lhadi, Photocatalytic degradation of azo-dyes reactive black 5 and reactive yellow 145 in water over a newly deposited titanium dioxide, Appl. Catal. B 57 (2005) 55–62.
[10] B.E. Barragán, C. Costa, M. Carmen Márquez, Biodegradation of azo dyes by bacteria inoculated on solid media, Dyes Pigm. 75 (2007) 73–81.
[11] G. McKay, J.F. Porter, G.R. Prasad, The removal of dye colors from aqueous solutions by adsorption on low-cost materials, Water Air Soil Pollut. 114 (1999) 423–438.
[12] S. Baup, C. Jaffre, D. Wolbert, A. Laplanche, Adsorption of pesticides onto granulated activated carbon: Determination of surface diffusivities using simple batch experiments, Adsorption 6(3) (2000) 219–228.
[13] V.K. Gupta, A. Suhas, Application of low-cost adsorbents for dye removal review, J. Environ. Eng. 90 (2009) 2313–2342.
[14] J. Mittal, V. Thakur, A. Mittal, Batch removal of hazardous azo dye Bismark Brown R using waste material hen feather, Ecol. Eng. 60 (2013) 249–253.

[15] A. Mittal, V. Thakur, J. Mittal, H. Vardhan, Process development for the removal of hazardous anionic azo dye Congo red from wastewater by using hen feather as potential adsorbent, Desalin. Water Treat. 52(1–3) (2014) 227–237.
[16] J. Mittal, V. Thakur, A. Mittal, Batch removal of hazardous azo dye Bismark Brown R using waste material hen feather, Ecol. Eng. 60 (2013) 249–253.
[17] H. Daraei, A. Mittal, M. Noorisepehr, F. Daraei, Kinetic and equilibrium studies of adsorptive removal of phenol onto eggshell waste, Environ. Sci. Pollut. Res. 20 (2013) 4603–4611.
[18] H. Daraei, A. Mittal, M. Noorisepehr, J. Mittal, Separation of chromium from water samples using eggshell powder as a low-cost sorbent: Kinetic and thermodynamic studies, Desalin. Water Treat. 53(1) (2015) 214–220.
[19] H. Daraei, A. Mittal, J. Mittal, H. Kamali, Optimization of Cr(VI) removal onto biosorbent eggshell membrane: experimental & theoretical approaches, Desalin. Water Treat. 52(7–9) (2014) 1307–1315.
[20] R. Jain, P. Sharma, S. Sikarwar, J. Mittal, D. Pathak, Adsorption kinetics and thermodynamics of hazardous dye Tropaeoline 000 unto Aeroxide Alu C (Nano alumina): A non-carbon adsorbent, Desalin. Water Treat. 52(40–42) (2014) 7776–7783.
[21] J. Mittal, D. Jhare, H. Vardhan, A. Mittal, Utilization of bottom ash as a low-cost sorbent for the removal and recovery of a toxic halogen containing dye eosin yellow, Desalin. Water Treat. 52(22–24) (2014) 4508–4519.
[22] Y.C. Çengeloglu, E. Kır, M. Ersoz, Removal of fluoride from aqueous solution by using red mud, Sep. Purif. Technol. 28 (2002) 81–86.
[23] V.K. Gupta, M. Gupta, S. Sharma, Process development for the removal of lead and chromium from aqueous solutions using red mud—An aluminium industry waste, Water Res. 35 (2001) 1125–1134.
[24] J. Pradhan, S.N. Das, R.S. Thakur, Adsorption of hexavalent chromium from aqueous solution by using activated red mud, J. Colloid Interface Sci. 217(1) (1999) 137–141.
[25] S. Wang, H.M. Ang, M.O. Tadé, Novel applications of red mud as coagulant, adsorbent and catalyst for environmentally benign processes, Chemosphere 72(11) (2008) 1621–1635.
[26] A. Tor, Y. Cengeloglu, Removal of congo red from aqueous solution by adsorption onto acid activated red mud, J. Hazard. Mater. 138 (2006) 409–415.
[27] V.K. Gupta, Suhas, I. Ali, V.K. Saini, Removal of rhodamine B, fast green, and methylene blue from wastewater using red mud, an aluminum industry waste, Ind. Eng. Chem. Res. 43 (2004) 1740–1747.
[28] G.M. Ratnamala, K.V. Shetty, G. Srinikethan, Removal of Remazol Brilliant Blue Dye from dye contaminated water by adsorption using red mud: Equilibrium, kinetic and thermodynamic studies, Water Air Soil Pollut. 223 (2012) 6187–6199.
[29] S. Saadat, A. Karimi-Jashni, Optimization of Pb(II) adsorption onto modified walnut shells using factorial design and simplex methodologies, Chem. Eng. J. 173 (2011) 743–749.
[30] V. Gómez, M. Callao, Modeling the adsorption of dyes onto activated carbon by using experimental designs, Talanta 77 (2008) 84–89.
[31] K.J. Cronje, K. Chetty, M. Carsky, J.N. Sahu, B.C. Meikap, Optimization of chromium(VI) sorption potential using developed activated carbon from sugarcane bagasse with chemical activation by zinc chloride, Desalination 275 (2011) 276–284.
[32] S. Agatzini-Leonardou, P. Oustadakis, P.E. Tsakiridis, Ch. Markopoulos, Titanium leaching from red mud by diluted sulfuric acid at atmospheric pressure, J. Hazard. Mater. 157 (2008) 579–586.
[33] J.S. Shing, Method of activation of red mud, US Patent 4017425, (1997).
[34] O. Regina Ajemba, Modification of the physico-chemical properties of udi clay mineral to enhance its adsorptive capacity, Adv. Appl. Sci. Res. 3(4) (2012) 2042–2049.
[35] C. Namasivayam, R. Yamuna, D. Arasi, Removal of acid violet from wastewater by adsorption on waste red mud, Environ. Geol. 41 (2001) 269–273.
[36] Ö. Gerçel, H.F. Gerçel, A.S. Koparal, Ü.B. Öğütveren, Removal of disperse dye from aqueous solution by novel adsorbent prepared from biomass plant material, J. Hazard. Mater. 160 (2008) 668–674.
[37] F. Rozada, L.F. Calvo, A.I. Garcia, J. Martin-villarcota, M. Otero, Dye adsorption by sewage sludge-based activated carbons in batch and fixed-bed systems, Bioresour. Technol. 87 (2002) 221–230.
[38] Z. Aksu, G. Dönmez, A comparative study on the biosorption characteristics of some yeasts for Remazol Blue reactive dye, Chemosphere 50 (2003) 1075–1083.